Synthesis and Photoelectrochemical Activity of TiO₂ Nanotube Based Free Standing Membrane

MISRIYANI[1,*],[ID] and E.S. KUNARTI[2,][ID]

[1]Medical Education, Faculty of Medicine, University of Alkhairaat, Jl. Diponegoro Palu 94221, Central Sulawesi, Indonesia
[2]Department of Chemistry, Faculty of Mathematics and Natural Sciences, Universitas Gadjah Mada, Sekip Utara, P.O. BOX BLS 21, Yogyakarta 55281, Indonesia

*Corresponding author: E-mail: misriyani85@gmail.com

TiO₂ nanotubes (TNTs) were synthesized and modified using the anodization method in a glycerol and ammonium fluoride solution, which was followed by a thermal treatment. The second anodisation was continued by increasing anodizing voltage to deposit a film on the surface of titanium, which resulted in a free standing membrane based on of TNTs. The nanotubes were further characterised using X-ray diffraction (XRD), scanning electron microscopy (SEM), and Fourier transform infrared (FTIR) spectroscopy. The SEM result showed that the layer thickness of free standing membrane based on TNTs increased with an increase in the anodizing voltage; however, at high voltages, this layer was damaged. The XRD and FTIR results indicated the generation of TNT having an anatase crystal phase. The results of test for photoelectrochemical properties showed that the optimal conditions of anodizing voltage was 50 V maintained for 1 h.

Keywords: TiO₂ nanotube, Free standing membrane, Anodization, Photoelectrochemical.

INTRODUCTION

Since 1972, when Fujishima and Honda presented the decomposition of water on exposure to light by employing TiO₂ photoelectrode, TiO₂ performance has been widely investigated to study its efficiency in photoelectrochemistry. To improve its efficiency, photoelectrochemical cell configurations and TiO₂ semiconductor materials were developed [1]. The TNTs fabricated though anodisation provide relatively better photocatalytic properties for photoelectrodes because they exhibit a one-dimensional channel for charge transfer and large surface area to reduce the recombination of holes (h⁺) and electrons (e⁻) [2]. Recent developments include the production of TNTs on a titania foil by varying anodization process conditions, such as annealing temperature, influence of water composition, temperature, anodization time and voltage of anodization, for their photoelectrochemical application under exposure to ultraviolet (UV) light [3-5]. The fabricated nanotubes were characterized to determine the change in their morphology caused by the influence of anodising voltage. The photoelectrochemical activities of TiO₂ membranes were investigated.

The free standing membrane film based on TNTs is highly effective for producing hydrogen through water splitting; however, the presence of titanium substrates is a barrier to the response of light. The morphology of TNTs present on titanium substrates was opaque, which limited the amount of light that falling on the TiO₂ surface, thereby affecting photocatalytic reduction reactions employed for hydrogen production. This study synthesized and modified TNT films having a standalone membrane without titanium substrates (free standing membrane) to achieve a membrane that can directly transfer electrons, be easily integrated with other substrates and remain stable against vibrations [6].

The photoelectrochemical activity of free-standing TNT membranes in hydrogen production and impacts of anodization voltage were investigated. A relationship between the photoelectrocatalytic performance of TNT-based free-standing membranes and synthesis conditions in hydrogen production was explored.

EXPERIMENTAL

The free standing TiO₂ nanotube membranes were prepared by anodization method of titanium foils (Baoji Jinsheng metal

material Co., purity 99.6%, thickness 0.3 mm) using ethylene glycol 98% (Merck), 25% water and ammonium fluoride (Merck) as electrolyte solution.

General procedure: The synthesis of free standing TiO_2 nanotube membrane was conducted in two step anodization procedure by preparing two electrodes, Titanium plate on anode cell and Pt wire on cathode cell connected to DC-Power Supply. Both electrodes are dipped in glycerol solution containing NH_4F 0.5% and water 25%. The anodizing process produces a bubble of hydrogen gas in the surroundings Pt wire at a voltage of 50 V and accompanied by stirring for 1 h [4,5,7,8]. After the anodization, the obtained TiO_2 plate is then rinsed slowly, dried up and calcined at 500 ºC for 3 h to obtain TiO_2 nanotube crystalline. Furthermore, annealed TiO_2 nanotube were anodized again to obtain free standing TiO_2 nanotube membrane by increasing the anodizing voltage at 60 V for 10 min under the same electrolyte conditions [9].
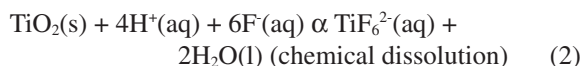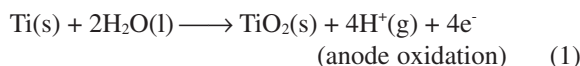
Detection method: The morphology of free standing TiO_2 nanotube membranes surface were investigated using field emission scanning electron microscopy (FESEM, FEI-Inspect F50 with accelerating voltage of 20 kV), the crystalline structure was measured using an X-ray diffraction instrument with Cu Kα radiation at 40 kV and 30 mA (Maxima.X Shimadzu), FTIR analysis of TiO_2 was performed using KBR pellet method at wavenumber 4000-400 cm^{-1} (FTIR PC Shimadzu) to study the functional groups in the photocatalyst. The photoelectrochemical activity measurements were performed using eDAQ Potensiostat (model ED401) connected to photoelectrochemical reactor consisting of counter electrode, reference electrode and the source of illumination (GNB 11W UV lamp). The results of photoelectrochemical analysis were recorded on computer with echem software.

RESULTS AND DISCUSSION

Electrochemical mechanism: In an electrolyte solution, TNTs were produced using two electrodes through electrochemical anodisation, in which a titanium foil and Pt wire serve as an anode and counter electrode, respectively. TNT formation begins with metal surface oxidation, which leads to the release of electrons and Ti^{4+} ions. An oxide is generated on the metal surface acquired through chemical dissolution that causes the release of Ti^{4+} ions and O_2^- or OH^- ions are obtained from water. Hydrogen gas evolution indicates the formation of titanium oxide obtained from anodisation through condensation on the Pt cathode surface.

The initial stage of anodizing process is the electrochemical oxidation on the surface of titanium and establish a uniform array TiO_2 nanotubes on the titanium surface according to the eqns. 1 and 2 [10]:

$$Ti(s) + 2H_2O(l) \longrightarrow TiO_2(s) + 4H^+(g) + 4e^-$$
$$\text{(anode oxidation)} \quad (1)$$

$$TiO_2(s) + 4H^+(aq) + 6F^-(aq) \; \alpha \; TiF_6^{2-}(aq) +$$
$$2H_2O(l) \; \text{(chemical dissolution)} \quad (2)$$

Titania nanotube growth results from a competition between chemical dissolution and anode oxidation in the electrolyte solution having fluoride. In an electric field, titanium hexafluoride forms, which leads fluoride ions (F^-) and TiF_6^{2-} to move toward the metal and electrolyte, respectively (eqn. 3):

$$Ti^{4+}(s) + 6F^-(aq) \longrightarrow TiF_6^{-2}(aq) \quad (3)$$

A barrier layer present at the metal/oxide interface of nanotube films acts as a barrier to the flow of ions (Ti^{4+} and O_2), which must flow through the film to continue anodic oxidation. Ti-O bonds polarize and weaken, which caused metal cation dissolution. Ti^{4+} ions travel from the metal to oxide/electrolyte interface and then dissolve in the electrolyte solution of HF. Free anions O_2^- migrate to the metal/oxide interface and subsequently interact with metals. By increasing the anodization voltage, a large barrier can be overcome. The TNT length increases until the rates of oxidation and chemical dissolution reactions occurring at the metal/oxide interface and top of tube (oxide/electrolyte), respectively, attain equilibrium. After equilibrium, the tube length does not depend on the anodization voltage.

Effect of anodizing voltage

SEM analysis: Fig. 1 illustrates the lengths of TNT films prepared at various anodising voltages. The length of TNT films increased at anodization voltage of 40-50 V and exhibited a stable layer structure (no damage). The length of TNT films did not vary substantially at the anodisation voltage of 60 V, and at this voltage, the TNT film layer was damaged. This finding indicated that an increase in anodizing voltage results in electrochemical etching to accelerate tube formation, which was observed by increasing nanotube lengths [11,12].

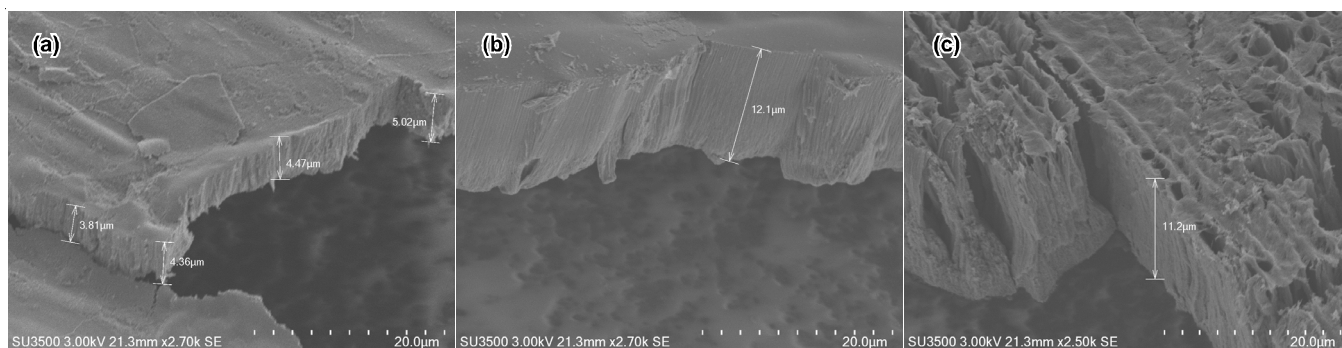However, at high anodixing voltage, tube lengths did not increase and the TNT film layer was damaged. The increased

Fig. 1. Photographic FESEM characterization of cross-sectional view of TiO_2 nanotubes (a) 40V (b) 50 V and (c) 60 V on a titanium foil

tube length influenced a large active surface area of TiO₂, which affected the increasing response to current provided by TNTs. Thus, an optimum condition of anodizing voltage must be achieved to obtain long TNTs. The optimum anodizing voltage used was 50 V for further synthesis.

XRD analysis: Fig. 2 presents the XRD patterns of TNT membranes obtained at various anodising voltage. According to the JCPDS data, the characteristic peak of the TiO₂ anatase crystal appeared at 2θ 25, 68º (001); 38, 1º (004); 39, 16º (112); and 48, 79º (020).

For the TNT samples obtained at anodization voltage of 40, 50 and 60 V, the characteristic anatase peaks appeared at 2θ of 30º (d011); 79º (d004); 57º (d112); and 08º (d020). This results are accurate as the characteristic peaks of TiO₂ [13,14]. However, at 40 V, the characteristic peak did not appear clearly at 68º probably because of the incomplete TiO₂ anatase crystal formation.
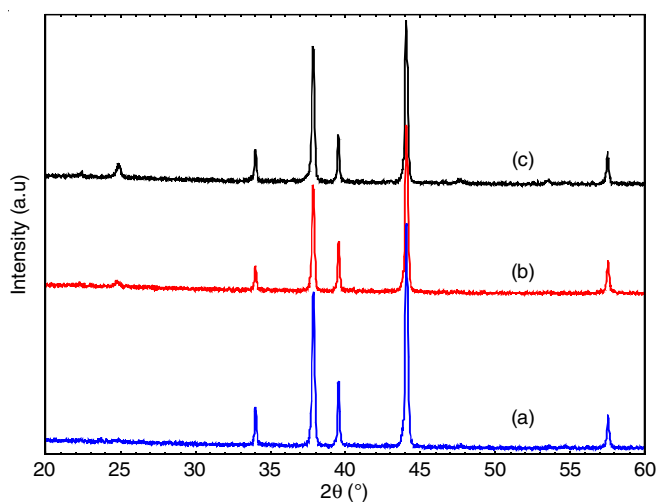
Fig. 2.   X-ray diffractogram of free standing TiO₂ nanotube membrane anodized at voltage: (a) 40 V (b) 50 V and (c) 60 V

At 60 V, the intensity of TNT anatase crystals became higher and sharper with an increase in the anodizing voltage. At high voltages, the tube was damaged; however, an increase in tube length led to increased intensity. The growth of nanotube thickness could enhance the anatase peak intensity [15]. The increase in anodization voltage resulted in electrochemical etching, which accelerated tube formation and can be observed from the increasing length and diameter of nanotubes. The large surface area of TNTs present in materials also have influences on it.

FTIR analysis: Fig. 3 presents the FT-IR spectra of the free-standing TNT membrane acquired to identify its functional groups. The IR spectra illustrate the influence of the anodisation voltage on synthesis with transmission peaks obtained in the wavenumber of 4000-400 cm⁻¹. The transmission peak appearing at 420 cm⁻¹ was the characteristic peak for Ti-O-Ti stretching vibration in TiO₂ crystals. The highest vibration frequency of Ti-O-Ti bonds was observed in TNTs anodized at 50 V (486.62 cm⁻¹). For the free-standing TNT membrane anodized at 40 V and 60 V, the vibration frequency decreased towards lower wavenumber (462.92
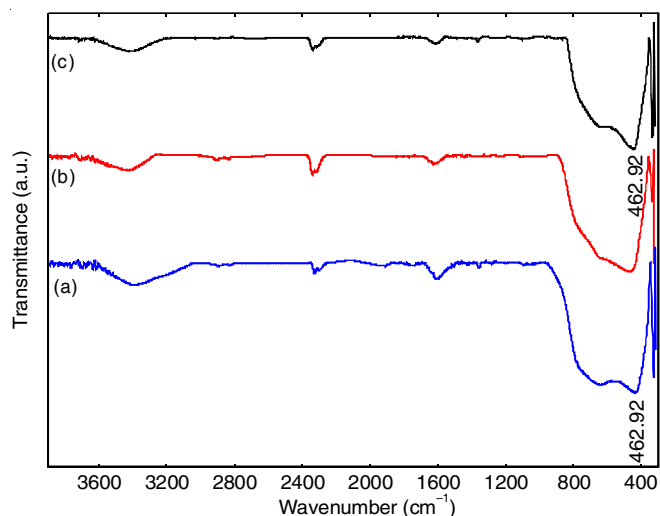
Fig. 3.   FT-IR spectra of free standing TiO₂ nanotube membrane anodized at voltage: (a) 40 V, (b) 50 V and (c) 60 V

cm⁻¹). A wavenumber shift towards a higher value indicated the Ti-O-Ti bond strength; thus, this bond requires a large amount of energy for vibration. Energy is directly proportional to wavenumber values. Moreover, IR peaks appearing at 2300 cm⁻¹ showed that the surface activity associated with the crystalline form of anatase was increasing [16]. Ti-O-Ti bonds with perfect crystals were formed at 50 V. By contrast, the transmission peaks appearing at the wavenumbers of 1620 and 3394 cm⁻¹ corresponded to the bending and stretching vibrations of the hydroxyl bonds of water molecules that were trapped on the TiO₂ surface.

Photoelectrochemical activity test: Fig. 4 presents the photocurrent curves employed to estimate the light response of the free-standing TNT membranes prepared at different anodization voltage. The increase in anodisation voltage (40 to 50 V) was in line with the increase in the photocurrent response to light. This finding indicated that the increase in anodization voltage expedites electrochemical etching to form tubes and increases the tube diameter and length [11,12]. The anodization voltage influences the increasing surface area of TiO₂, which

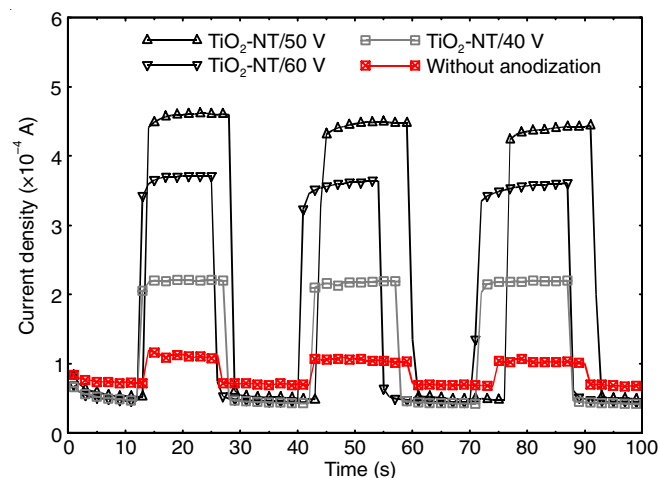Fig. 4.   Photocurrent response of free standing TiO₂ nanotube membrane with multi pulse amperometry techniques under UV light exposure

affects increasing light response. A decrease in the photocurrent response of TNTs at 60 V results in changes in pores with random structures and damage to nanotubular structures [17].

Conclusion

Free-standing TNT membranes can be prepared through two steps of anodization. The synthesis optimum conditions were obtained at 50 V followed by the thermal treatment (500 ℃). This finding was supported by the increase in the photo-electrochemical activity as a response to light.

CONFLICT OF INTEREST

The authors declare that there is no conflict of interests regarding the publication of this article.

REFERENCES

1. D. Wei and G. Amaratunga, *Int. J. Electrochem. Sci.*, **2**, 897 (2007).
2. X. Pan, Q. Xie, W. Chen, G. Zhuang, X. Zhong and J.J. Wang, *Int. J. Hydrogen Energy*, **38**, 2095 (2013);
   https://doi.org/10.1016/j.ijhydene.2012.11.115
3. Misriyani, A.W. Wahab, P. Taba and J. Gunlazuardi, *Int. J. Appl. Chem.*, **11**, 611 (2015).
4. L. Li, Z. Zhou, J. Lei, J. He, S. Zhang and F. Pan, *Appl. Surf. Sci.*, **258**, 3647 (2012);
   https://doi.org/10.1016/j.apsusc.2011.11.131
5. J. Kapusta-Kolodziej, O. Tynkevych, A. Pawlik, M. Jarosz, J. Mech and G.D. Sulka, *Electrochim. Acta*, **144**, 127 (2014);
   https://doi.org/10.1016/j.electacta.2014.08.055
6. G. Liu, T. Chen, Y. Sun, G. Chen and K. Wang, *Appl. Surf. Sci.*, **311**, 529 (2014);
   https://doi.org/10.1016/j.apsusc.2014.05.104
7. R. Liu, W.D. Yang, L.S. Qiang and J.F. Wu, *Thin Solid Films*, **519**, 6459 (2011);
   https://doi.org/10.1016/j.tsf.2011.04.231
8. Ratnawati, J. Gunlazuardi, E.L. Dewi and Slamet, *Int. J. Hydrogen Energy*, **39**, 16927 (2014);
   https://doi.org/10.1016/j.ijhydene.2014.07.178
9. A.M.D. Fornari, M.B. de Araujo, C.B. Duarte, G. Machado, S.R. Teixeira and D.E. Weibel, *Int. J. Hydrogen Energy*, **41**, 11599 (2016);
   https://doi.org/10.1016/j.ijhydene.2016.02.055
10. A. Robin, M.B. de Almeida Ribeiro, J.L. Rosa, R.Z. Nakazato and M.B. Silva, *J. Surf. Eng. Mater. Adv. Technol.*, **04**, 123 (2014);
    https://doi.org/10.4236/jsemat.2014.43016
11. A.-K. M.A. Alsamuraee, Q.M.D. Al-Ittabi and Y.A. Mohammed, *Am. J. Sci. Ind. Res.*, **2**, 852 (2011).
12. M. Nischk, P. Mazierski, M. Gazda and A. Zaleska, *Appl. Catal. B*, **144**, 674 (2014);
    https://doi.org/10.1016/j.apcatb.2013.07.041
13. J. Zhang, R.G. Du, Z.Q. Lin, Y.F. Zhu, Y. Guo, H.Q. Qi, L. Xu and C.J. Lin, *Electrochim. Acta*, **83**, 59 (2012);
    https://doi.org/10.1016/j.electacta.2012.07.120
14. Misriyani, E.S. Kunarti and M. Yasuda, *Indones. J. Chem.*, **15**, 43 (2015);
    https://doi.org/10.22146/ijc.21222
15. S. Bauer, A. Pittrof, H. Tsuchiya and P. Schmuki, *Electrochem. Commun.*, **13**, 538 (2011);
    https://doi.org/10.1016/j.elecom.2011.03.003
16. A. Henegar and T. Gougousi, *J. Solid State Sci. Technol.*, **4**, 298 (2015);
    https://doi.org/10.1149/2.0041508jss
17. H. Omidvar, S. Goodarzi, A. Seif and A.R. Azadmehr, *Superlattices Microstruct.*, **50**, 26 (2011);
    https://doi.org/10.1016/j.spmi.2011.04.006